PRAMANA
— journal of
physics

Vol. 59, No. 6
December 2002
pp. 1061–1073

A high resolution AMS-injector for the Pelletron in Lund

R HELLBORG[1], S BAZHAL[2], M FAARINEN[1], K HÅKANSSON[1],
C-E MAGNUSSON[1], P PERSSON[1], G SKOG[1] and K STENSTRÖM[1]
[1]Department of Physics, Lund University, Sölvegatan 14, SE-223 62 LUND, Sweden
[2]SSC RF Institute for Physics and Power Engineering, 1, Bondarenko Sq., Obninsk,
Kaluga Region, 249033, Russia

Abstract. A high resolution injector system has recently been installed at the Lund 3 MV tandem Pelletron accelerator. The new injector, designed mainly for ^{26}Al ions, will increase the experimental potential of the Lund AMS facility considerably. High quality energy- and mass-resolution is obtained by using a 90° spherical electrostatic analyzer followed by a 90° magnetic analyzer. The injector is equipped with a high intensity sputtering source with a spherical ionizer.

A new analytical technique for acceptance calculations as well as PC-based computational methods have been used in the design of the ion optical system of the new injector.

Compared to our old injector system which has a magnetic analyzer with a bending angle of only 15°, the new system has a more than ten times better resolution. The beam optics of the new system is also better designed to match the accelerator acceptance. In this way the ion transmission from the ion source to the detector, for different ions of interest in our AMS programme, has been increased.

Keywords. AMS; ion optical system; Pelletron; electrostatic accelerator; accelerator mass spectrometry; injector.

PACS No. 29.17

1. Introduction

An important advantage of a tandem electrostatic accelerator as compared to a single-ended machine is the easy access to the ion source, e.g. for maintenance and when the ion species is to be changed. A tandem also provides the possibility of having different sources installed in different injector legs. The major drawbacks of a tandem accelerator are: the need for a negative ion source which in general produces significantly lower ion currents as compared to a positive source; and the increase of the beam emittance due to scattering when the beam passes the terminal stripper medium [1]. It is therefore of great importance – especially when doing experiments that make high demands on the ion beam – to have a well-designed optical system from the ion source to the accelerator. The low-energy system must be able to transport the beam from the source aperture to the accelerator with minimal loss and to produce an emittance area which will match the accelerator acceptance area. Finally, together with the low energy accelerator tube, it must be able to produce a beam cross-over at the stripper. A cross-over at the stripper position will result in a minimum increase of the beam emittance area when the beam passes the stripper medium [2].

The original optics of the low energy system of the 3 MV Pelletron tandem accelerator in Lund was designed for light ions such as protons, deuterons and helium ions. This simple optical system was redesigned in the middle of the 80's when requirements grew for experiments with medium–heavy ions. By using simple, beam optical calculations [3], the low energy system was improved considerably. The new design made it possible to obtain a beam cross-over at the stripper for light ions as well as for medium–heavy ions, and the transmission through the accelerator for the medium–heavy ions increased by about a factor of four. This redesign was a prerequisite for new experiments such as AMS [4], isotope production for medical purposes [5] and – at that time – the PIXE micro-beam [6]. The simple calculations on the beam envelope, described in ref. [3], were later followed by more detailed studies [7,8] of the existing optics. The latter calculations included space charge effects as well as an accurate description of the distribution of the potential in the region of the ion source extraction. A new recursive technique [9,10] was used in these studies to solve the equations of motion for charged particles.

Despite the redesign described above, a serious limitation of the existing low energy system still remained, in that the original inflection magnet is single focusing and has a bending angle of only 15°. This magnet is the only mass separating unit between the source and the accelerator. The limited resolution became apparent some years ago when ion masses heavier than ^{14}C were introduced into our AMS program [4]. It was therefore decided to add a new injector with good energy and mass separation and procure a high current ion source. Our biomedical program with ^{26}Al ions [11] provides the main impetus for the development and installation of the new injector. However, the new injector will also be advantageous for our program for detecting ^{59}Ni in nuclear waste material [12]. In this paper we report on the design of the new injector, the optical calculations and the experimental test of the system. Preliminary reports of the optical design [13,14], a description of the analytical technique used [15], as well as a detailed technical description of the installation [16] can be found elsewhere.

2. Design of the new injector

The old injector of the Lund Pelletron consists of two injector legs. One leg is used for an off-axis duoplasmatron mainly for the production of H^- ions. The other leg is used for the production of many different types of ions from solid materials, using an in-house built sputtering source of the Cs-gun type [17,18]. This source was developed several years ago for use in our AMS program. The two injector legs are connected to the two 15° ports of the inflection magnet. As mentioned above there are serious drawbacks, especially for heavier ions, due to the poor mass resolution of this magnet inherent in the small deflection angle, and the fact that the magnet focuses only in the bending plane.

To obtain better mass and energy separation – which is especially important in AMS experiments – the new injector system has been developed. A schematic diagram of the new system is shown in figure 1. The new injector includes a 90° double focusing magnet (for best mass separation) and a 90° spherical electrostatic analyzer (for best energy separation). By using a spherical analyzer, double focusing is also provided by this unit. The importance of including an energy analyzer is to reduce contributions from the energy tails of neighbouring masses. The ion source in the new injector is a high current, spherical ionizer, sputtering source.

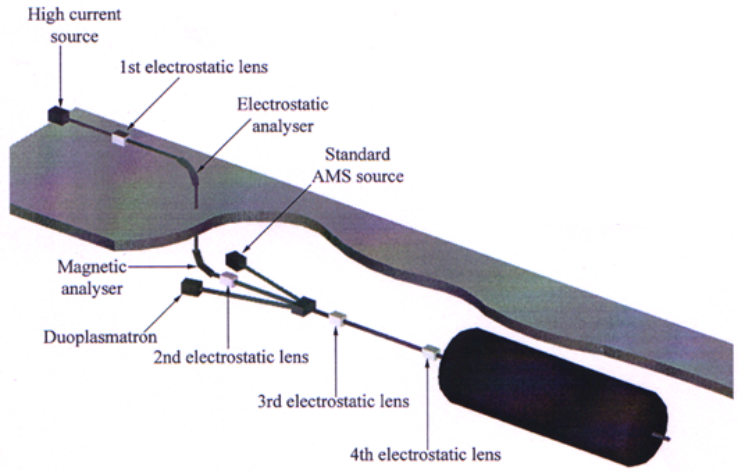

Figure 1. The layout of the new injector, together with the two old injectors and part of the accelerator. Dark boxes – ion sources, light boxes – electrostatic lenses.

As can be seen in figure 1 the new ion source is placed at an elevated level compared to the existing injectors and accelerator system. This is motivated by the severe space limitations in the existing injector hall, which made it impossible to accommodate the new injector at that level. The new injector is connected to the 0°-port of the old inflection magnet.

The 90° double focusing magnet (of uniform field, with a pole edge rotation of 28.2°, a bending radius of 373.5 mm and a vacuum gap in the non-dispersive plane of 39 mm) and the 90° spherical electrostatic analyzer (with a bending radius of 435 mm, and spacing between plates 43.5 mm) were both delivered by Danfysik, Jyllinge, Denmark. The two electrostatic quadrupole triplet lenses (aperture diameter 65 mm) and the sputtering ion source were obtained from the Niels Bohr Institute at Risø, Denmark, as they were available due to the termination of their FN tandem programme and the shutting down of that machine. With the exception of the equipment obtained from Denmark, the whole injector has been designed and built at our institute. A detailed drawing of the injector is shown in figure 2. In the beam cross-over plane just after the source lens, a beam profile monitor, followed by a beam stop, is positioned. This plane is the object plane of the first electrostatic quadrupole triplet. In the image plane of this lens a four-blade, changeable aperture followed by a beam stop is placed. This plane is also the object of the electrostatic analyzer. In the image plane of the electrostatic analyzer (which is also the object plane of the 90° magnet) a two-blade, changeable aperture, followed by a beam stop, is located. The last aperture (also with two blades) is placed in the image plane of the 90° magnet. This plane is also the object plane of the second electrostatic quadrupole triplet.

A pressure in the range of 10^{-5}–10^{-6} Pa is obtained by three pumps. A 1500 l/s cryogenic pump is placed just after the ion source lens, a similar cryopump is connected to the chamber of the electrostaic analyzer and finally a 3100 l/s diffusion pump is placed just after the 90° magnet. The vacuum chamber of the magnet is electrically insulated, giving the possibility to quickly change the mass injected into the accelerator by changing the potential of the chamber. Three steerers, for the angular corrections of the beam, are included

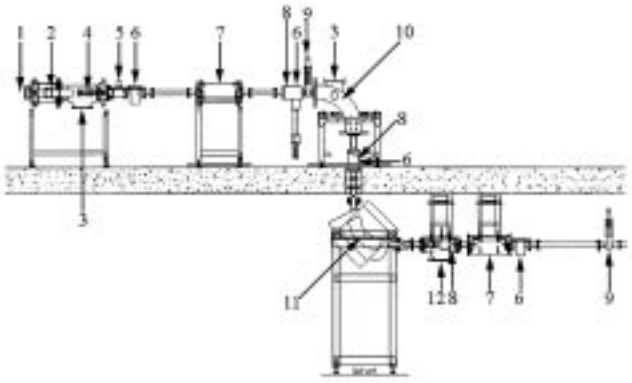

Figure 2. A drawing of the new injector. Numerals: 1 – Position of the ion source, 2 – Einzel lens, 3 – position of cryogenic pump, 4 – electrostatic steerer, 5 – beam scanner, 6 – Faraday cup, 7 – electrostatic quadrupole triplet, 8 – slits, 9 – valve, 10 – electrostatic energy analyzer, 11 – magnetic mass analyzer, 12 – diffusion pump.

in the installation, an xy-steerer just after the source lens, a second steerer downstream of the electrostatic analyzer, steering in the non-dispersive plane of the analyzer, and finally one steerer just after the 90° magnet, steering in the non-dispersive plane of the magnet.

3. Calculations for the optics

At the design stage we carried out calculations on the ion optics of the new injector. The calculations were aimed at the choice of the placement for the lens elements in the ion optical channel as well as at the development of a new lens for the sputtering ion source. The new optics were to meet the following requirements: (1) to transport the beam through the system with minimal loss, (2) to produce an ion beam cross-over at the stripper and (3) to achieve a better energy and mass resolution compared to the old system. A two-level layout of the new injector was determined by the restrictions due to the construction of the building. As a result, the position of the analyzer section relative to the 0°-port of the old magnet could not be chosen arbitrarily. It should also be mentioned, that the maximum length of the beam line on the upper level was restricted by the distance between the electrostatic analyzer and the opposite wall of the injector room. Taking these circumstances into account, we began the calculations.

At the initial stage we used a first-order approach to simulate the optical system of the new injector. The choice of calculation technique was determined by the application of lenses with axially symmetrical electrostatic field (i.e. the ion source lens, the Einzel lens, the aperture lens). A description of the transverse motion of the charged particles in terms of the transport matrices involves some difficulties for these elements. Therefore, a method based on the numerical solution of a system of differential equations for the beam envelopes with Kapchinskiy–Vladimirskiy density distribution was used [13]. Making use of Picht's substitution [19] allowed us to exclude the second derivative of the axial potential from the equations

$$\begin{cases} R_x'' = k\frac{I}{W(R_x+R_y)} + \frac{W_0 E_x^2}{R_x^3} - \frac{3}{16}\left(\frac{W'}{W}\right)^2 R_x \pm \omega_x^2 R_x \\ R_y'' = k\frac{I}{W(R_x+R_y)} + \frac{W_0 E_y^2}{R_y^3} - \frac{3}{16}\left(\frac{W'}{W}\right)^2 R_y \pm \omega_y^2 R_y \end{cases} \tag{1}$$

where W denotes the kinetic energy of the axial particle in eV with an initial value of W_0, I is the beam current in Amperes and $E_{x,y}$ denotes the beam emittance in m·rad. The coefficient k is defined by eq. (2):

$$k = \frac{Z_{\mathrm{i}}}{2\pi\varepsilon_0}\sqrt{\frac{A}{2\eta_p}}, \tag{2}$$

where Z_{i} is the charge state of the ion, A is the mass number of the ion, $\varepsilon_0 = 8.85 \cdot 10^{-12}$ F/m and $\eta_p = 0.958 \cdot 10^8$ C/kg. The relation between the beam envelope $r_{x,y}$ and the variable $R_{x,y}$ is given by the Picht's substitution $r_{x,y} = R_{x,y}W^{-0.25}$.

The coefficients ω_{xy}^2 describe the focusing $(-)$ and defocusing $(+)$ effect of the linear ion optical elements. For different elements of the low energy system the coefficients ω_{xy}^2 have the following values and expressions:

Drift space: $\omega_{xy}^2 = 0$.

Axial symmetric electrostatic field: $\omega_{xy}^2 = 0$.

Electrostatic quadrupole lens: $\omega_{xy}^2 = Z_{\mathrm{i}}V/a^2W$, where V is the voltage applied to the lens electrodes in volts and a is the aperture radius of the lens.

Magnetic analyzer: $\omega^2 = (1-n)/\rho_m^2$ in the dispersive plane, $\omega^2 = n/\rho_m^2$ in the non-dispersive plane, where n is a field index and ρ_m is the bending radius.

Spherical electrostatic analyzer: $\omega^2 = 1/\rho_e^2$ in the dispersive plane, $\omega^2 = 1/\rho_e^2$ in the non-dispersive plane and ρ_e is the bending radius.

In the framework of this method the electrostatic field was determined by the numerical solution of Dirichlet's problem. The integral equation technique was used for the field calculation. The continuous distribution of the axial potential was approached by a cubic spline. A superposition technique was applied to describe the electrostatic field in the multielectrode lenses. A PC code was developed for the numerical solution of eq. (1). This software allows us to consider the optical system of the electrostatic accelerator as consisting of an arbitrary set of the elements mentioned above. Both numerical and graphical representations of the results obtained are possible.

Improvement of the energy and mass separation in the new injector can be in contradiction with beam transport conditions through the analyzer section. Indeed, to obtain better ion separation in the analyzers one needs to use the slits with narrow aperture, which can result in beam losses due to a decrease in the acceptance of the analyzers. We investigated the conditions of the beam transport through the analyzers, making use of the first-order analytical calculation techniques [15]. An expression for the estimation of the upper limit of the slit opening S, necessary to separate the ions of interest with mass m_0 from the neighboring masses $m_0 + \Delta m$ was found:

$$S \leq \frac{2\rho_e\rho_m}{2\rho_e(1-\tan\beta)+\rho_m}\frac{|\Delta m|}{m_0} \tag{3}$$

where β denotes an angle between the principal trajectory of the ion in the magnetic analyzer and the normal to the effective field boundary (i.e. an angle of the pole edge rotation). For example, substituting $\rho_m = 0.3735$ m, $\rho_e = 0.435$ m, $\beta = 28.2^\circ$ and $|\Delta m| = 1$ in eq. (3) yields $S \leq 7$ mm for ^{59}Ni ions. This estimation gives the maximum opening (7 mm) of the slits to provide the necessary mass separation. To compare the acceptance of the analyzers and the beam emittance we assumed that slits with an opening of 6 mm are used. Taking into account the transverse dimensions of the vacuum chambers in the dispersive (YOZ) and non-dispersive (XOZ) planes ($2r_y = 43.5$ mm for the electrostatic analyzer; $2r_y = 80$ mm and $2r_x = 39$ mm for the magnetic analyzer) we calculated the acceptance of the two analyzers. The calculation yields the following values: acceptance of the electrostatic analyzer $A_y = 106$ mm·mrad; acceptances of the magnetic analyzer $A_y = 105$ mm·mrad and $A_x = 73$ mm·mrad. A comparison of these acceptances with the emittance of the spherical ionizer, sputtering ion source (equal to 29 mm·mrad for the beam energy of 42 keV) permitted us to conclude that the ion transport through the analyzers is possible without appreciable losses. More detailed acceptance calculations carried out taking into account the orientation of the phase ellipses can be found in ref. [15].

A program for medical and biological research at the accelerator mass spectrometer in Lund includes ^{26}Al measurements. To carry out the measurements it is necessary to have a beam of negative ions of aluminium at a current in the range of 1–2 μA. The production of negative ions in this range encounters some difficulties in aluminium due to its small electron affinity (0.46 eV). It would be advantageous instead of Al^-, to accelerate AlO^-, which is more easily produced. To do so, it is necessary to completely strip the ions before detection, which requires an energy higher than that available at the Lund AMS facility. A multiple sample, sputtering ion source has been used for some years in radiocarbon measurements [17,18], but this source does not provide the necessary current for an Al beam. It was therefore decided to install in the new injector line a spherical ionizer ion source [20], which can produce more intensive negative ion beams.

According to our design, the beam has to be focused in a waist at the entrance of the ion optical channel of the new injector. The ion source lens, in the existing line of injection does not allow a convergent beam to be produced [8] and therefore cannot be used in the new design. A four-electrode layout with independently variable electrode potentials was chosen for the ion source lens. For the design of the lens we carried out the ion optical calculation making use of the technique described in ref. [13].

It was assumed that a negative carbon ion beam was to be used to test the system before its routine operation. All calculations below were done for carbon ions. We calculated the beam envelopes for that part of the ion optical system between the spherical ionizer (figure 2, part 1) and the beam scanner, positioned at a distance of 620 mm from the accelerating electrode (figure 2, part 5) of the lens in the plane of the beam waist. Experimental values of the beam emittance, published in ref. [21] were utilized in the calculations. We have no quantitative information on the beam geometry at the exit aperture of the central hole of the ionizer. Therefore, several different values of the beam radius and divergence were considered as possible initial conditions for the beam envelope calculations. It was not known, which of these values would be the best approach to the real beam geometry. The calculations showed that the beam waist would be obtained at the beam scanner position for all of these initial values. However, the electrode voltages strongly depended upon the choice of geometry of the incoming beam. To give a more accurate definition of the initial conditions we simulated the ion beam in the sputtering source [22]. The beam envelope

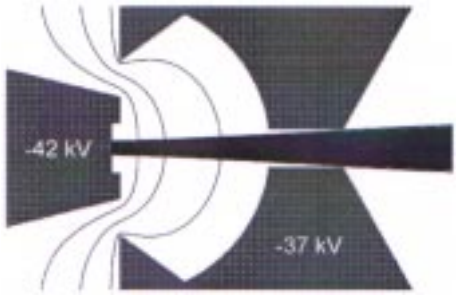

Figure 3. SIMION simulation of the C^- ion beam in the ionizer chamber of the spherical ionizer, sputtering ion source.

calculations by the method described in ref. [13] are carried out in the first-order approach. Consequently this method cannot be applied to ion sources in which the conditions of the beam paraxiality are not implemented. To simulate a beam in the ion source we made use of the program SIMION [23].

The finite difference method is used in the SIMION program for the numerical solution of the Laplace equation. SIMION is aimed at a wide range of ion optical problems. In particular, the program allows the user to 'construct' the beams with a given initial distribution as well as to take into account the space charge forces. The method of calculation assumes that the Coulomb field of the ion beam does not affect the external field created by the lens electrodes. Therefore, the ion current in the beam model has to be about ten times less than the Child's law constraint. It seems that this condition can be applied to the negative carbon ion beams with current in the range of 5–10 μA.

The joint model of the ion source, including the lens electrodes, was built on a 6011×501 grid with a step size of 0.1 mm. The axial symmetry of the system was taken into account in the model. The sputtering area (i.e. the area of negative ion emission) on the sample surface was assumed to have a diameter of 1.6 mm. This diameter is approximately twice the diameter of the actual crater created on the surface by the central part of the cesium beam. (The enlarged area of emission simulates the sample sputtering by a halo of the beam.) The angular distribution of the ions, emitted from the sample surface, was set up in accordance with experimental values of the beam emittance for the spherical ionizer, sputtering source [21]. The beam under consideration consisted of 200 particles distributed uniformly in the beam cross-section. The number of particles used in the model was limited by the time required for the calculation. It needed about 2 h to solve the problem for 200 ions on a PC (CPU Intel Pentium Celeron, 400 MHz).

4. Results of the calculations

The results of the simulation of the carbon ion beam in the ionizer chamber of the sputtering source are given in figure 3. The calculations were carried out for a fixed position of the sample holder. The beam current is equal to 10 μA, the normalized beam emittance is 4π mm·mrad$\sqrt{\text{MeV}}$ and the cathode and anode voltages are -42 and -37 kV, respectively. In our model these conditions provided the beam transport through the central hole of the ionizer practically without any losses. An emittance area for the beam cross-section

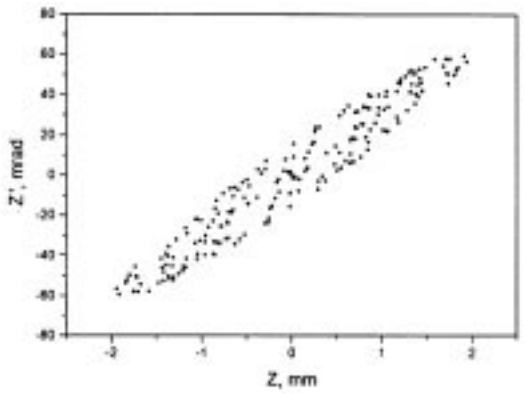

Figure 4. Diagram of the emittance at the exit aperture in the central hole of the spherical ionizer.

positioned at a distance of 39 mm from the sample surface is shown in figure 4. The calculated radius of the beam in this cross-section is 1.9 mm and the beam divergence is 56 mrad. (We have used these data as initial conditions for the calculation of the beam transport through the low energy side of the Lund Pelletron accelerator.) At the emittance value of 6π mm·mrad$\sqrt{\text{MeV}}$ the beam simulation resulted in ion losses at the walls of the ionizer channel. We did not carry out detailed calculations of the channel acceptance. However, the value of acceptance seems to be close to the emittance values mentioned above.

The beam geometry from the surface of the sputtering sample to the beam scanner positioned at the entrance to the injector is shown in figure 5. The same initial conditions as used for the calculations inside the ionizer chamber (figure 3) were introduced in the joint model of the source and the lens. We assumed the following voltages at the electrodes of the system: $U_1 = -42$ kV, $U_2 = -37$ kV, $U_3 = -31$ kV, $U_4 = -37$ kV, $U_5 = -22$ kV and $U_6 = 0$ kV. To compare the results obtained by the different techniques, the beam envelopes calculated by SIMION and found by the numerical solution of the envelope equations are shown in figure 6. The calculations were done for two values of the emittance, namely, 2π mm·mrad$\sqrt{\text{MeV}}$ (figure 6a) and 4π mm·mrad$\sqrt{\text{MeV}}$ (figure 6b). In both cases the results obtained by the two methods are in good agreement. Some differences between the beam geometry are observed. A plane of the beam waist calculated by SIMION has a small shift towards the lens. This can be explained by the influence of geometrical aberrations, which are not taken into account in the framework of the paraxial approach in the beam envelope method.

Beam envelopes in the low energy part of the Lund Pelletron accelerator, including the new injector and accelerating tube are illustrated in figure 7. The envelopes were found in the first-order approach by the numerical solution of eq. (1). Two carbon beams with currents of 5 and 10 μA and initial conditions obtained from the SIMION simulation were considered. In contrast to the calculations described in refs [14,22] the energy of injection was reduced to 40 keV. It is defined by the maximum voltage of the main power supply now in use in the new injector. We assumed that the following voltages were applied to the electrodes of the ion source and ion source lens (see figure 5): $U_1 = -40$ kV, $U_2 = -35$ kV, $U_3 = -29$ kV, $U_4 = -35.4$ kV, $U_5 = -20$ kV and $U_6 = 0$ kV. All voltages except U_4 are

Figure 5. C^- beam simulation in the ion source section of the new injector. Numerals: 1 – cathode of the sputtering ion source, 2 – spherical ionizer, 3 – entrance electrode of the lens, 4 – focusing electrode, 5 – pre-accelerating electrode, 6 – accelerating electrode.

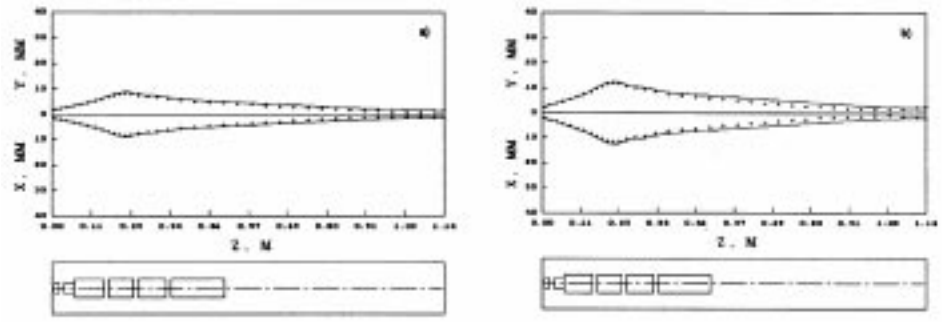

Figure 6. C^- beam simulation in the ion source section of the new injector, found by different calculation techniques (+ – SIMIION simulation, — – beam envelopes method) for 2 emittance values. (**a**) 2π mm·mrad $(\mathrm{MeV})^{0.5}$; (**b**) 4π mm·mrad $(\mathrm{MeV})^{0.5}$.

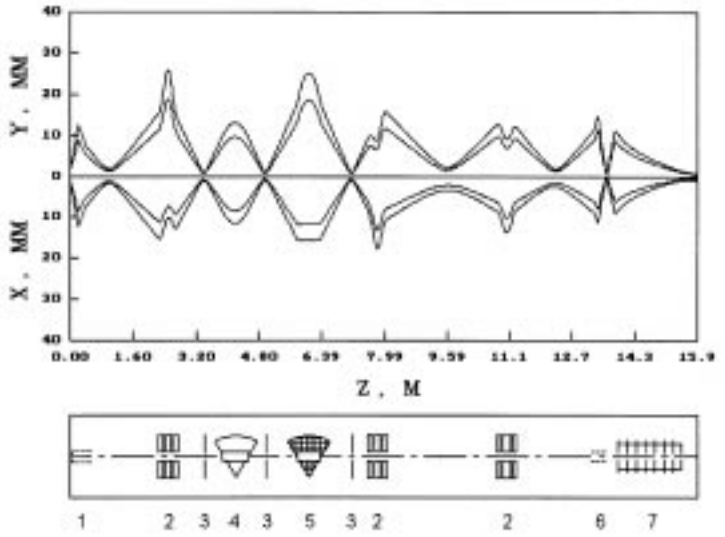

Figure 7. Beam envelopes in the low energy part of the Lund Pelletron accelerator. Calculations were carried out for two carbon ion beams with an energy of 5 keV at the starting point and injection energy of 40 keV ($I = 5\,\mu$A, $\varepsilon = 2\pi$ mm·mrad$\sqrt{\mathrm{MeV}}$, $r_0 = 1.4$ mm, $r_0' = 0.04$ and $I = 10\ \mu$A, $\varepsilon = 4\pi$ mm·mrad$\sqrt{\mathrm{MeV}}$, $r_0 = 1.9$ mm, $r_0' = 0.056$). Numerals: 1 – ion source lens, 2 – electrostatic quadrupole triplet, 3 – slit device, 4 – spherical electrostatic analyzer, 5 – magnetic analyzer, 6 – Einzel lens, 7 – accelerating tube.

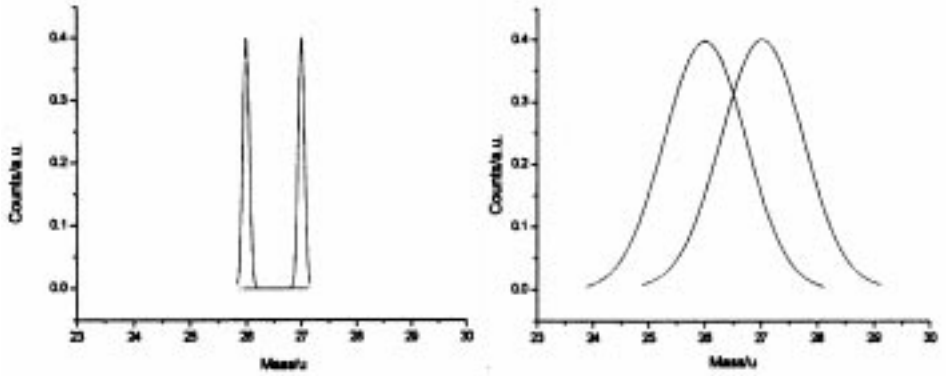

Figure 8. Resolution of the 90° electrostatic and the 90° magnetic analyzers (left) compared to the resolution of the 15° magnetic analyzer (right).

similar to those found from our first experience with running the ion source. (U_4 in the tests was varied from –35.6 kV to –36.4 kV depending mainly on the sputtering conditions.)

The results obtained illustrate the beam transport through the low energy part of the accelerator. The introduction of the new ion source lens now allows the beam to be formed into a waist on the first beam scanner. The voltages calculated for the lens electrodes are in agreement with their experimental values. In the two transversal planes the beam emittance can be matched to the analyzer acceptance. In the dispersive plane of the analyzers, where the beam size at the slits cannot be arbitrarily increased, the beam in these calculations occupies approximately half of the vacuum chamber. We expect limited transport conditions in the non-dispersive plane of the magnetic analyzer. However, the transversal dimension of the beam in this case does not exceed the chamber constrains. Moreover, the transport conditions can be improved by increasing the initial size of the beam, as there are no essential restrictions on the beam along the input slit of the analyzer. And finally, the ion optical system of the new injector provides the conditions necessary to match the beam emittance with the acceptance of the accelerating tube and to have a beam waist at the position of the stripper.

5. Experimental tests and discussion

Experimental study of ion optical properties of the new injector has just begun. Preliminary tests show that the resolution of the new injector with the 90° electrostatic and 90° magnetic analyzers compared with the existing injector with a 15° magnetic analyzer is greater by more than a factor of 10. A test with nickel samples shows that all the isotopes of nickel (i.e. 58, 60, 62 and 64) are individually identifiable, whereas with the old injector they are bundled together. For aluminium the troublesome isobar MgH^- will be completely suppressed. This is illustrated in figure 8. The injector is designed for the whole periodic system, although for heavy masses $(m > 230)$ it is not possible to use the insulated magnetic chamber for switching masses.

First ion optical measurements at the new injector have been carried out. We studied some focusing regimes of the ion source lens. A beam profile obtained by the scanner (part

5 in figure 2) for one of the regimes is given in figure 9. The profile was taken under the following conditions: ion species – carbon, unanalyzed beam current – 16 μA, voltages, applied to the lens electrodes (see figure 5): $U_1 = -40$ kV, $U_2 = -35$ kV, $U_3 = -19.8$ kV, $U_4 = -34$ kV, $U_5 = -20$ kV and $U_6 = 0$ kV. The beam envelopes calculated under the same conditions are shown in figure 10.

Figure 9. Beam focusing by the ion source lens. The beam profile (lower part of the photo) was obtained for the following voltages, applied to the lens electrodes: $U_1 = -40$ kV, $U_2 = -35$ kV, $U_3 = -19.8$ kV, $U_4 = -34$ kV, $U_5 = -20$ kV and $U_6 = 0$ kV. (The upper part of the photo shows the trigger signal from the profile monitor to the oscilloscope.)

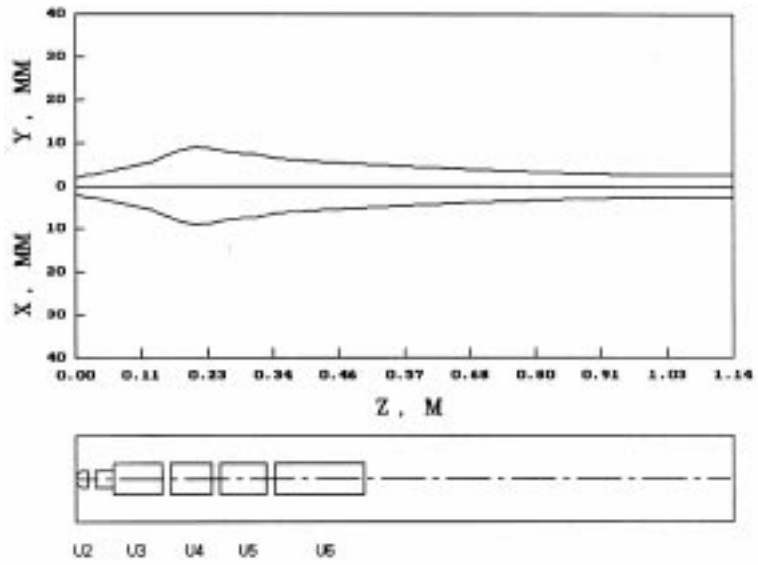

Figure 10. Beam envelopes calculated under the same voltage and beam conditions as those which have been used in the measurements presented in figure 9.

The distance between the sample and the ionizer marked 1 and 2 in figure 5 has been shown to be crucial for the optimization of the current. Therefore, a mechanical construction has been installed which provides the possibility of changing the distance while the voltages are maintained.

In the ion source there is a position for one sample only. If the aim is only to optimize the ion current during an evaluation procedure this is sufficient. The sample can be changed in 10 min with the vacuum maintained. When AMS measurements are to be done, it would be advantageous to have the possibility to change samples with maintained vacuum and high voltages on the sample. Therefore, a redesign of the ion source with a multi-sample wheel is being considered.

References

[1] U A S Tapper, R Hellborg and K G Malmqvist, *Nucl. Instrum. Methods* **B34**, 407 (1988)

[2] P Tykesson, H H Andersen and J Heinemeier, *IEEE Trans.* **NS-23 (2)** 1104 (1976)

[3] R Hellborg, K Håkansson and G Skog, *Nucl. Instrum. Methods* **A287**, 161 (1990)

[4] R Hellborg, L Curtis, B Erlandsson, M Faarinen, M Kiisk, C-E Magnusson, G Skog and K Stenström, *Phys. Scr.* **61**, 530 (2000)

[5] T Ohlsson, A Sandell, R Hellborg, K Håkansson, C Nilsson and S-E Strand, *Nucl. Instrum. Methods* **A379**, 341 (1996)

[6] K G Malmqvist, L Asking, H-C Hansson, R Hellborg, G Hyltén, E-M Johansson, S A E Johansson, P Kristiansson, P Larsson, N E G Lövestam, B G Martinsson, J Pallon, B Svantesson, E Swietlicki, U A S Tapper and K Themner, *Nucl. Instrum. Methods* **B40/41**, 685 (1989)

[7] A Dymnikov, R Hellborg, J Pallon, G Skog, C Yang and G Ohlén, *Nucl. Instrum. Methods* **A328**, 164 (1993)

[8] A Dymnikov, R Hellborg, J Pallon, G Skog and C Yang, *Nucl. Instrum. Methods* **A334**, 266 (1993)

[9] A Dymnikov and R Hellborg, *Nucl. Instrum. Methods* **A330**, 323 (1993)

[10] A Dymnikov and R Hellborg, *Nucl. Instrum. Methods* **A330**, 343 (1993)

[11] M Faarinen, C-E Magnusson, R Hellborg, S Mattsson, M Kiisk, P Persson, A Schütz, G Skog and K Stenström, *J. Inorganic Biochem.* **87**, 57 (2001)

[12] P Persson, M Kiisk, B Erlandsson, M Faarinen, R Hellborg, G Skog and K Stenström, *Nucl. Instrum. Methods* **B172**, 188 (2000)

[13] S Bahzal, M Faarinen, R Hellborg, C-E Magnusson and V Romanov, *Proc. 13th Int. Conference on Electrostatic Accelerators*, Obninsk, Russia, 25–28 May 1999, p. 160

[14] R Hellborg, S Bazhal, M Faarinen and C-E Magnusson, *Proc. 1999 Symposium of Northeastern Accelerator Personnel*, Knoxville, Tennessee, 25–28 October 1999, p. 83

[15] R Hellborg, M Faarinen, C-E Magnusson, S V Bazhal and V A Ronanov, *Nucl. Instrum. Methods* **A465**, 297 (2001)

[16] M Faarinen, R Hellborg, M Kiisk, C E Magnusson, P Persson, G Skog, K Stenström, S Bazhal, *Proc. 2001 Symposium of Northeastern Accelerator Personnel*, Lund, Sweden, 22–25 October 2001, p. 10

[17] K Håkansson, R Hellborg, B Erlandsson, G Skog, K Stenström and A Wiebert, *Nucl. Instrum. Methods* **A382**, 327 (1996)

[18] P Persson, K Freiman, R Hellborg, K Håkansson, G Skog and K Stenström, *Rev. Scientific Instrum.* **69**, 1188 (1998)

[19] A P Banford, *The transport of charged particle beams* (London, Spon, 1966)

[20] M Faarinen and C-E Magnusson, Evaluation of a spherical ioniser ion source for Al-ions, Report 09/00 LUNFD6, Lund University, Lund, 2000

[21] G D Alton *et al*, *Nucl. Instrum. Methods* **B24/25**, 826 (1987)
[22] S V Bazhal and R Hellborg, *Proc. 14th Int. Conf. on Electrostatic Accelerators and Beam Technologies*, Obninsk, Russia, 6–9 June 2001 (in press)
[23] D A Dahl, SIMION 3D Vers. 6.0 User's manual, Idaho National Engineering Laboratory INEL-95/0403, 1995